



**HAL**  
open science

**The evolution of the deep flow regime at  
Soultz-sous-Forêts, Rhine Graben, eastern France:  
Evidence from a composite quartz vein**

M. Smith, V. Savary, B. Yardley, J. Valley, Jean-Jacques Royer, Michel Dubois

► **To cite this version:**

M. Smith, V. Savary, B. Yardley, J. Valley, Jean-Jacques Royer, et al.. The evolution of the deep flow regime at Soultz-sous-Forêts, Rhine Graben, eastern France: Evidence from a composite quartz vein. *Journal of Geophysical Research : Solid Earth*, 1998, 103 (B11), pp.27223-27237. 10.1029/98JB02528 . hal-04044545

**HAL Id: hal-04044545**

**<https://hal.univ-lorraine.fr/hal-04044545v1>**

Submitted on 31 Mar 2023

**HAL** is a multi-disciplinary open access archive for the deposit and dissemination of scientific research documents, whether they are published or not. The documents may come from teaching and research institutions in France or abroad, or from public or private research centers.

L'archive ouverte pluridisciplinaire **HAL**, est destinée au dépôt et à la diffusion de documents scientifiques de niveau recherche, publiés ou non, émanant des établissements d'enseignement et de recherche français ou étrangers, des laboratoires publics ou privés.

Copyright

## The evolution of the deep flow regime at Soultz-sous-Forêts, Rhine Graben, eastern France: Evidence from a composite quartz vein

M. P. Smith,<sup>1,2</sup> V. Savary,<sup>3</sup> B. W. D. Yardley,<sup>1</sup> J. W. Valley,<sup>4</sup> J. J. Royer,<sup>3</sup> and M. Dubois<sup>5</sup>

**Abstract.** Drilling at Soultz-sous-Forêts, France, conducted as part of the European Hot Dry Rock Project, intersected a fracture lined with vein quartz and actively producing hot (150°C) water at 2174 m depth in the granite basement to the Rhine Graben. At least seven generations of quartz are present within the vein, but fluid inclusion homogenization temperatures show that temperatures remained within 15°C of the present field temperature throughout its development, apart from a few rare pulses of hotter water. In contrast, freezing measurements indicate two distinct fluids. The more saline one, ranging from 10 to 15 wt % NaCl eq, dominated the early stages of vein fill, while the second, ranging from 0 to 8 wt % NaCl eq, become more prominent in later stages. Oxygen isotope analyses of different quartz generations also show two populations in addition to magmatic relicts. In the early stages a population with  $\delta^{18}\text{O}$  from 14‰ to 18‰ predominates and is consistent with growth from a sedimentary basin brine. Later quartz shows lighter values (12‰–13‰), resulting from precipitation from a fluid isotopically identical to the modern fluid, which is in equilibrium with granite feldspar at a temperature ~25°C higher than the present vein temperature. The change in  $\delta^{18}\text{O}$  does not, however, correlate with that in fluid salinity, reflecting the different effects of fluid-rock interaction on the two parameters. Changes in fluid salinity, possibly resulting from meteoric inputs into the deep formation waters of the Rhine Graben, occurred early in the flow path of the Soultz fluids because there is no decrease in fluid temperature associated with even the most dilute inclusion fluids. With time the path by which these fluids from deep in the Mesozoic sediments of the graben have made their way to the Soultz site has changed, resulting in greater interaction with granite, as recorded in the oxygen signature.

### 1. Introduction

Studies of contemporary deep fluid flow in crystalline basement rocks are important both for the insight that they give into the development of hydrothermal rocks and veins from the geological record and for their direct relevance to geothermal energy and deep waste disposal. Despite the low matrix permeability of such rocks the fracture permeability may be high [Brace, 1980], and fluxes of often saline aqueous fluids have been reported flowing through granitic basement in several areas [e.g. Fritz and Frape, 1987]. The area around Soultz-sous-Forêts in the Rhine Graben, Alsace, France, was selected for the site of the European Hot Dry Rock Project [Bresee, 1992] because of the high geothermal gradient [Gérard and Kappelmeyer, 1987], which probably results

from upwelling of hot fluids from depth [Clauser, 1989]. In the past this region has been exploited for petroleum in the Oligocene Pechelbronn Series. Geothermal research drilling at Soultz began in 1987. Three deep holes penetrate the basement, GPK-1, GPK-2, and EPS-1 (Figure 1), and of these EPS-1 was cored continuously from 980 to 2230 m. Drilling has produced fluid with a slight artesian flow from within the granite basement in EPS-1 [Pauwels *et al.*, 1993], and such circulation was also observed during deepening of the GPK-1 and GPK-2 holes down to 3580 m [Elsass *et al.*, 1995]. These results are in agreement with the anomalous thermal gradient recorded from the drill holes.

The geochemical and isotopic characteristics of the deep fluid [Pauwels *et al.*, 1993] and the presence of organic matter in the associated altered granite [Ledésert *et al.*, 1993] indicate that the fluid now flowing through the granite was sourced in the younger Mesozoic sediments. Dubois *et al.* [1996] showed that the fluid inclusions present in veins from both granite and overlying sediments in the EPS-1 borehole were trapped at temperatures close to those measured down hole at the present time, but reveal a complex history of changing fluid chemistry. In hole EPS-1 the main deep fluid production was from an open fracture in granite at 2174 m depth. This fracture was within a composite zone of vein quartz over 50 cm in length (zone K195, cores 4780 and 4781) containing sporadic included rock fragments. This vein thus provides a link between present and past fluid flow and vein growth, and for this study we have investigated the texture of the vein for evidence of its history, then studied fluid inclusions and the oxygen isotopic composition of the quartz itself to understand how the fluid composition and temperature of the Soultz

<sup>1</sup>Department of Earth Sciences, University of Leeds, Leeds, U.K.

<sup>2</sup>Now at Department of Mineralogy, The Natural History Museum, London, England, U.K.

<sup>3</sup>Centre de Recherches Pétrographiques et Géochimiques - Centre National de la Recherche Scientifique, Vandoeuvre les Nancy Cedex, France.

<sup>4</sup>Department of Geology and Geophysics, University of Wisconsin, Madison.

<sup>5</sup>Université des Sciences et Technologies de Lille, Unité de Recherche Associée 719, Sédimentologie et Géodynamique - Villeneuve d'Ascq Cedex, France.

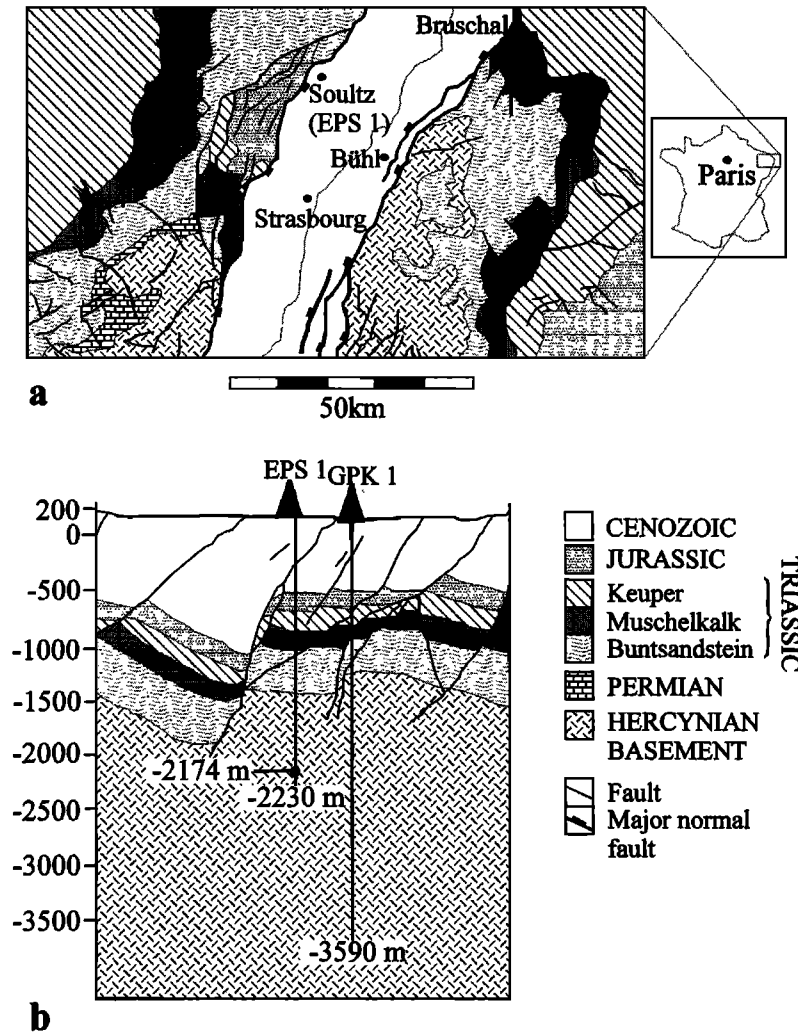


Figure 1. Location of the study site: (a) Map of the Rhine graben and its environs, indicating major geological units and the location of the drill site at Sultz-sous-Forêts and (b) cross section of the drill site [after Ledesert *et al.*, 1996].

hydrothermal system in the deep Rhine graben evolved through to the present day.

## 2. Geological Setting

### 2.1. Regional geology

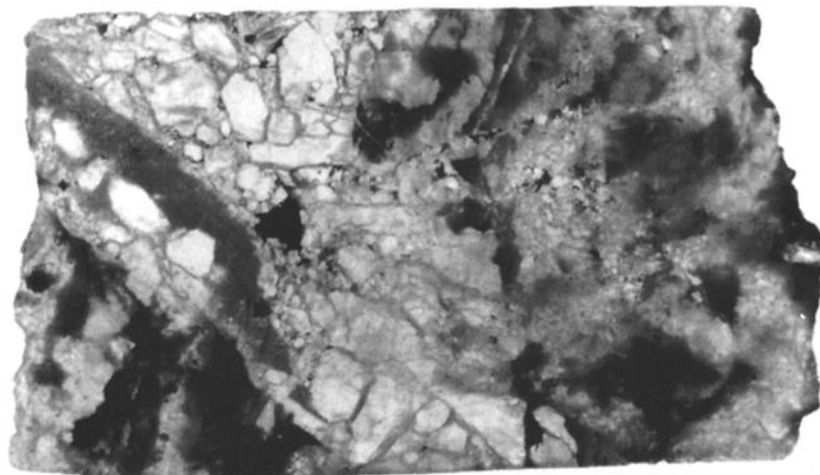
The Sultz-sous-Forêts area is located in the western part of the Upper Rhine Graben, ~50 km north of Strasbourg (Figure 1). The Rhine Graben is a major continental rift stretching from Basel (Switzerland) in the south to Frankfurt (Germany) in the north, and is believed to have formed during the Alpine orogeny [Illies and Greiner, 1978; Villemin *et al.*, 1986]. It is filled by up to 3 km of synrift sediments ranging in age from mid-Eocene to Quaternary. These overlie pre-Alpine, Mesozoic sediments and their Hercynian basement. The graben is bounded by faults with strike lengths of up to several kilometers, with Hercynian crystalline massifs (the Vosges and the Black Forest) and their overlying sediments (the Paris Basin and the Jura Mountains) to the east and west.

The EPS-1 borehole (Figure 1) encountered the unconformity between Permo-Triassic sediments and the Hercynian Sultz granite at 1400 m. GPK-1 reached a depth of

3590 m [Aquilina and Brach, 1995]. The Sultz granite consists of alkali feldspar phenocrysts in a matrix of quartz, plagioclase, biotite, and minor amphibole and is typical of Variscan granites as seen at the surface in the Vosges and Schwarzwald Massifs. It is altered in heavily fractured areas to clays with chlorite, corrensite, tosudite, carbonates, hematite, epidote, and rare hydrogarnet [Traineau *et al.*, 1991, Ledesert *et al.*, 1993; Komninou and Yardley, 1997]. Alteration may be accompanied by secondary quartz and K-feldspar and by a dramatic increase in porosity. Veins occur in many of the altered rocks and are of quartz, carbonates, or both, sometimes with barite, minor illitic white mica, or pyrite.




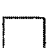




### 2.2. Modern Fluid Flow and the Sample Site.

Permeable zones have been encountered in the Sultz granite at depths of 1817, 1991, 2510, and 3490 m in well GPK-1 [Fouillac and Genter, 1991; Genter *et al.*, 1993; Aquilina and Brach, 1995], as well as at 2174 m in EPS-1. Saline fluid from the central opening of the vein in EPS-1 was at a temperature of 150°C, whilst that from 1820 m in the GPK-1 borehole was at a temperature of 137°C. Both fluids had salinities of ~10 wt % NaCl eq [Pauwels *et al.*, 1993].

**a**

1cm

**b**

- |  |   |
|--|---|
|  Stage 1: Nonluminescent quartz     |  Stage 4: Fine grained vuggy quartz                                    |
|  Stage 2: NLQ breccia matrix        |  Stage 5a and b: Vug filling quartz (outlines of major crystals shown) |
|  Phengite                           |  Stage 6: Microcrystalline quartz II                                   |
|  Stage 3: Microcrystalline quartz I |  Chalcopyrite  |

**Figure 2.** (a) Photograph of the polished surface of the sample wafer investigated in detail at Leeds and (b) Interpretation of the minerals and quartz generations illustrated in Figure 2a, based on cathodoluminescence imaging. The area highlighted by the dashed line is shown in detail in Figure 8.

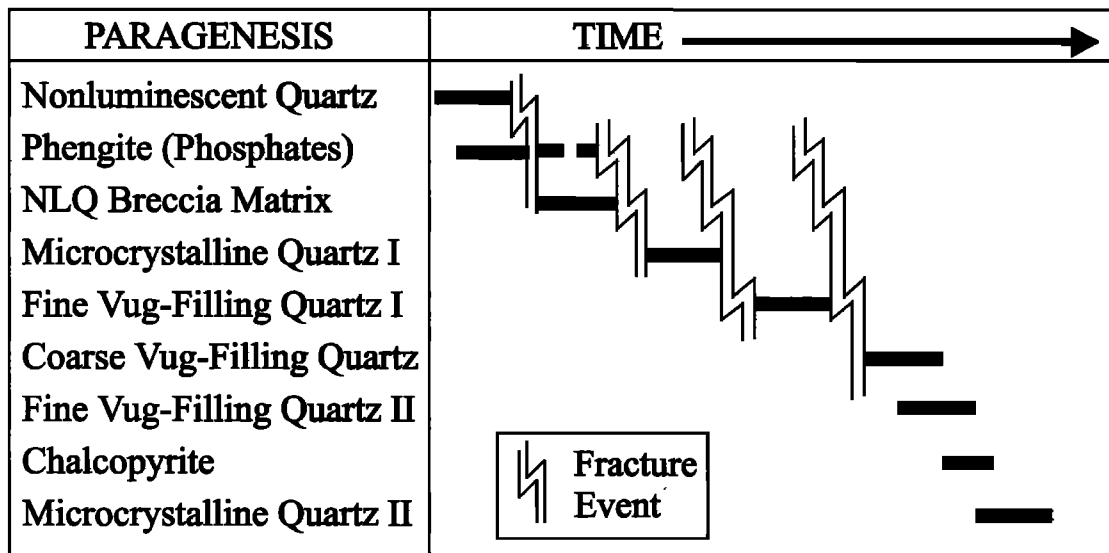
Previous analyses of fluid inclusions from this vein yielded a range of salinities, one higher than that of the modern fluid (14-16 wt % NaCl eq), another approximately equal to it (10-11 wt % NaCl eq), and a third that is less saline (~5 wt % NaCl eq) [Dubois *et al.*, 1996]. It is notable that a range of fluid salinities, including some very high values, are known from drilling into the Mesozoic sequence elsewhere in the Rhine Graben [Pauwels *et al.*, 1993].

For this study we made a detailed investigation of vein quartz from the central portion of the quartz vein at 2174 m in EPS-1. Separate pieces were investigated in Leeds and in

Nancy, but showed similar histories of quartz growth. Microthermometry was carried out on both pieces, and the material studied in Leeds was then broken up into small fragments for laser oxygen- isotope analysis at Madison.

### 3. Methods

Petrographic observations of the quartz generations were made by optical microscopy and, in the case of the sample piece studied in Leeds, by scanning electron microscope (SEM). The SEM observations were made in



**Figure 3.** Summary of the paragenesis and history of mineral growth in vein quartz from 2174 m in the EPS-1 drillcore.

cathodoluminescence (CL) and back scattered electron modes on a Camscan Series 4 SEM, operated at an accelerating voltage of 20 kV, and permitted distinction of impurity phases and precise recognition of quartz generations [cf. *Boiron et al.*, 1992]. Microthermometric measurements at Leeds were made using a Linkam TMS 90 heating-freezing stage, calibrated by use of a range of pure solids and a natural sample containing pure CO<sub>2</sub> inclusions. Microthermometric measurements were also made at the Centre de Recherches Pétrographiques et Géochimiques, Nancy, using a U.S. Geological Survey heating-freezing stage calibrated with synthetic fluid inclusions [*Dubois et al.*, 1996]. There is no systematic difference between data from the two laboratories, and the precision is estimated to be  $\pm 0.1^{\circ}$ - $0.2^{\circ}$ C near the freezing point of water and  $\pm 1^{\circ}$ - $2^{\circ}$ C at  $\sim 150^{\circ}$ C.

Following microthermometry and CL examination, the Leeds microthermometry wafer (Figure 2) was soaked for 48 hours in hexafluorosilicic acid to remove mica and carbonates. This also etched the surface of the sample so that the textural zones identified using CL could easily be distinguished using optical microscopy. The sample was broken into 61 distinct quartz fragments, each dominated by a single textural domain, which were analyzed for their oxygen isotope composition using laser fluorination at the University of Wisconsin, Madison [*Spicuzza et al.*, 1998]. The mass of each analyzed fragment was 1–2 mg and analyses of a single generation of coarse quartz ( $n = 9$ ) gave a precision of  $\sim 0.2\%$  ( $2\sigma$ ). Repeat analyses of standard UWG2 (Gore Mountain Garnet) gave a value of  $5.65\% \pm 0.2\%$  ( $2\sigma$ ;  $n = 8$ ), which compares well with the recommended value of  $5.8\%$  [*Valley et al.*, 1995], and so no further correction has been made. All analyses are given relative to SMOW.

#### 4. VEIN PETROGRAPHY

The vein investigated (Figure 2) is composed principally of quartz, with minor phengite, chalcopyrite, and carbonates and small ( $\sim 60$ - $<10\ \mu\text{m}$ ) rare crystals of apatite, monazite, and zircon, which were typically associated with the phengite. The

phengite may represent fragments of hydrothermally altered feldspar. Optically, the vein can be separated into regions of clear, vuggy, euhedral quartz, which overgrow zones of a cloudy, fine-grained quartz (the green quartz of *Dubois et al.* [1996]), commonly cut by veinlets of a clearer quartz generation. This fine-grained quartz commonly overgrows relict fragments of igneous quartz or heavily altered granite. These general relationships are clarified in CL and were used to compile a paragenetic sequence of quartz types for the sample examined by SEM-CL. The general relations of the different generations within the piece mapped using CL are shown in Figure 2, while the paragenetic sequence is summarized in Figure 3.

##### 4.1. Stage 1: Nonluminescent Quartz

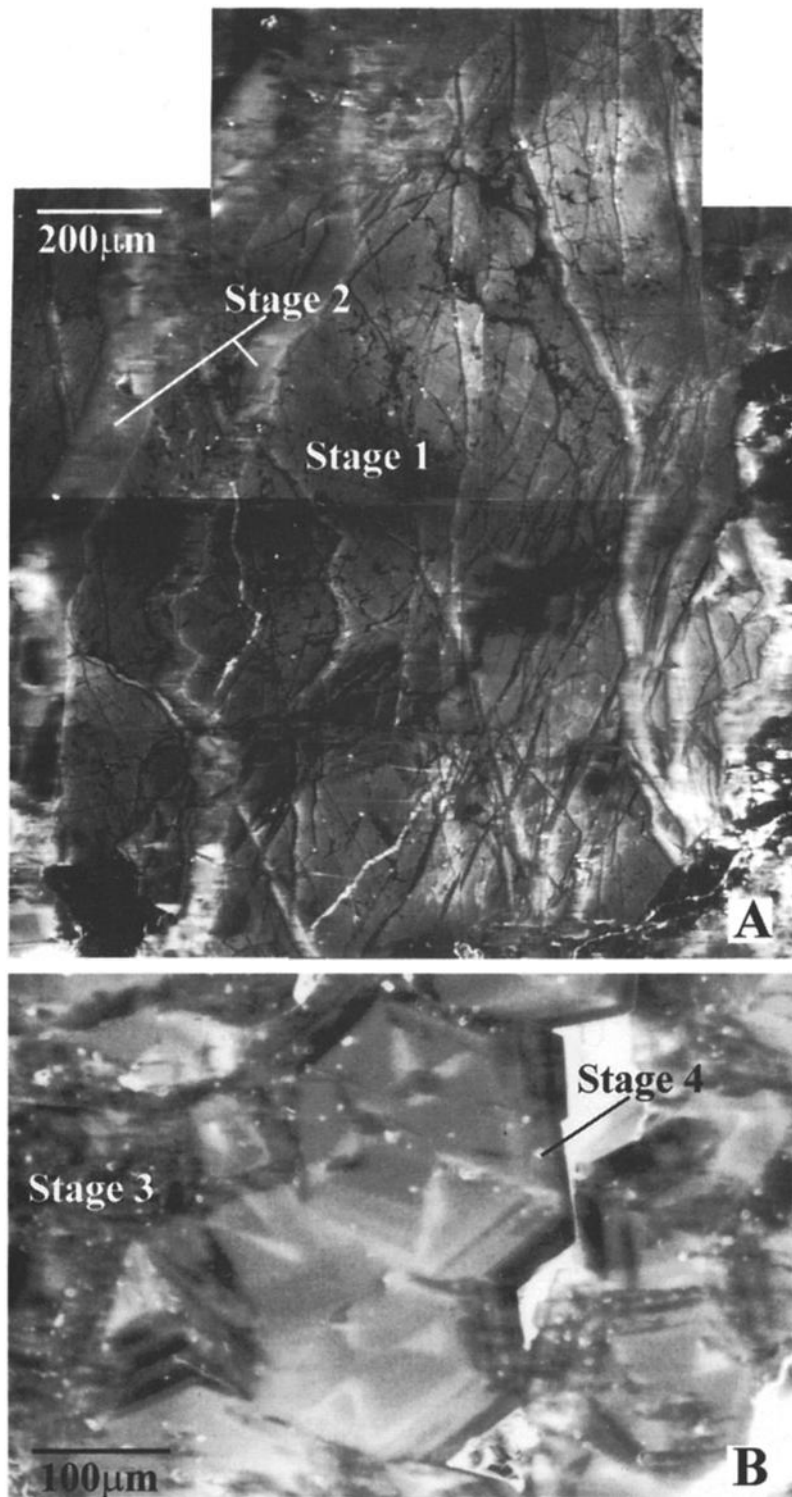
The earliest quartz generation is heavily fractured nonluminescent quartz (Figure 4), which occurs as large (0.5–1mm), angular fragments at the margins of the vein and as smaller ( $<0.3\ \text{mm}$ ) fragments in the vein center. It was identified as the earliest generation of quartz present as it is cut by virtually all of the fracture events recognized in the vein and occurs as inclusions in all the later generations of fracture fill.

##### 4.2. Stage 2: NLQ Breccia Matrix

A number of generations of fractures exist within the NLQ, the latest forming relatively wide zones of weakly luminescent quartz, which serve as a matrix to the breccia of nonluminescent quartz (Figure 4).

##### 4.3. Stage 3: Microcrystalline Quartz I

The brecciated NLQ underwent a second period of fracturing which formed large (0.2–0.5mm) composite fragments of NLQ and breccia matrix. These fragments are overgrown by zones of very fine grained (10–40 $\mu\text{m}$ ) quartz, here termed microcrystalline quartz, which occasionally include small grains of calcite. These zones correspond to the very cloudy to opaque quartz seen in Figure 2a.



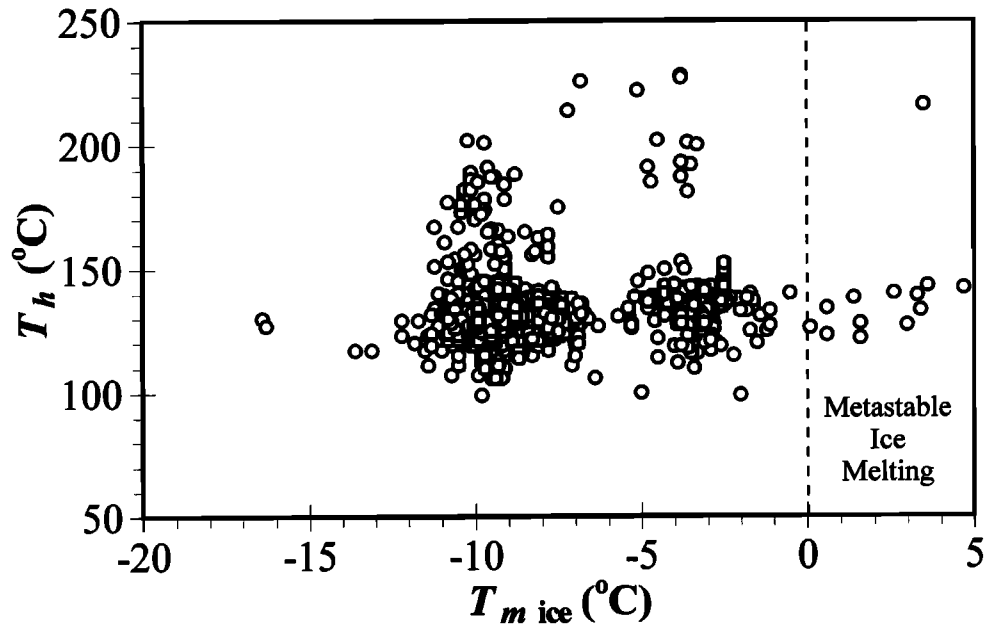
**Figure 4.** (a) Mosaic of cathodoluminescence (CL) images taken in the scanning electron microscope (SEM) to illustrate a brecciated fragment of nonluminescent quartz (stage 1) with many fine cracks sealed by secondary quartz growth (stage 2). (b) CL micrograph to illustrate oscillatory zoned fine-grained vuggy quartz grown into void space.

#### 4.4. Stage 4: Fine, Euhedral, Vuggy quartz I

The microcrystalline quartz and the NLQ breccia are, in turn, crosscut by a series of narrow (0.1-0.2 mm) fractures. These are infilled by fine-grained (100-300  $\mu\text{m}$ ), euhedral, vuggy quartz (Figure 4), which typically shows fine-scale internal oscillatory and sector zoning in CL.

#### 4.5. Stage 5: Central Vug Fill

All the previous generations are crosscut by the central zone of euhedral, vuggy quartz, which again shows oscillatory and sector zonation in CL. This zone has been subdivided into the coarse grained (1-2 mm) crystals (stage 5a: coarse-grained vug-filling quartz), which are surrounded by a coeval or a



**Figure 5.** Compilation of all microthermometric measurements from the quartz vein investigated in the present study. Note the markedly bimodal population of salinities and the strong clustering of homogenization temperatures close to the present temperature at 2174 m (see Figure 9). Of 1043 inclusions measured, 857 gave both  $T_h$  and  $T_{m \text{ ice}}$  values and are plotted here.

slightly later generation of fine-grained (100-500  $\mu\text{m}$ ) quartz (stage 5b: fine-grained vug-filling quartz II), with minor associated chalcopyrite.

#### 4.6. Stage 6: Microcrystalline Quartz II

The final quartz generation is a second generation of microcrystalline quartz which is coeval with, or slightly later than, the coarse-grained vug-filling quartz and can be seen to overgrow and fill the interstices between the coarse-grained euhedral crystals of stage 5a in Figure 2. Unfilled cavities remain.

Fluid inclusions within the vein are predominantly two-phase (L+V) aqueous inclusions ranging from 1 to 15  $\mu\text{m}$  in diameter, although a number of single phase (L) inclusions were observed. Many of the inclusions appear to be primary, and growth zones of fluid inclusions are apparent in the coarser quartz; however planes of secondary and pseudosecondary inclusions were also observed, and the data from these are recorded separately below. No fluid inclusions were observed in the microcrystalline quartz from stages 3 and 6.

## 5. FLUID INCLUSIONS

### 5.1. Microthermometry

The entire microthermometric data set from both laboratories is shown in Figure 5. The final melting temperature of ice in the inclusions ( $T_{m \text{ ice}}$ ) exhibits a broadly bimodal distribution, with the main groupings lying between -6.8° to -11.7°C and -2.0° to -4.0°C. Occasionally, the vapor bubble was eliminated by ice expansion on freezing and only reappeared on metastable ice melting at temperatures above 0°C [Roedder, 1967].  $T_{m \text{ ice}}$  was therefore only used to estimate fluid inclusion salinity if the vapor bubble was visible prior to final ice melting. The small size of the majority of

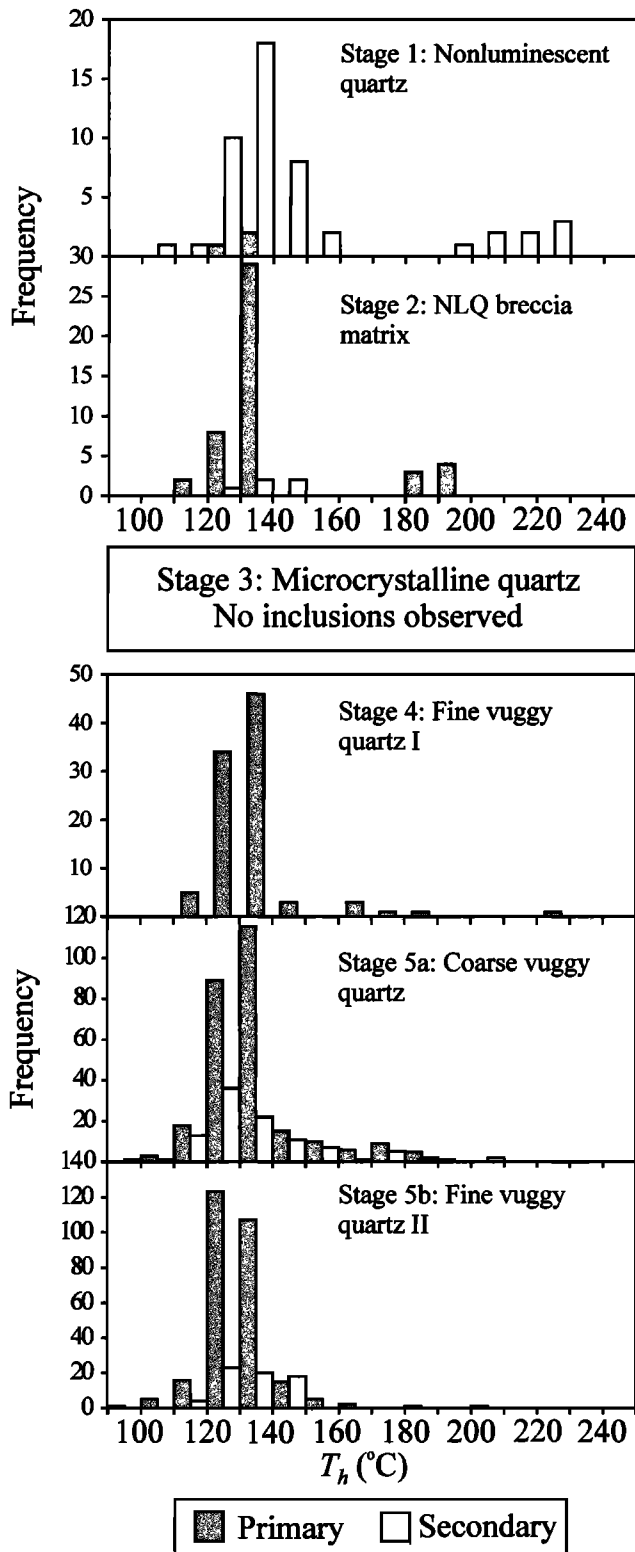
inclusions made eutectic temperatures difficult to observe, but a limited number of accurately observed first melting temperatures in the range -40°--56°C suggest a complex mix of salts in solution, with significant concentrations of divalent cations [cf. Pauwels *et al.*, 1993].

On heating, all the measured fluid inclusions homogenized to the liquid phase. The vast majority of the inclusions (78% of the data) gave homogenization temperatures ( $T_h$ ) between 120° and 145°C. A relatively small number of inclusions (10% of the data) homogenized at higher temperatures, ranging up to 228°C. These measurements agree closely with the earlier results of Dubois *et al.* [1996].

### 5.2. The Variation of Fluid Inclusion Properties with Quartz Generations

Histograms of  $T_h$  for each of the quartz generations identified using CL are shown in Figure 6, and histograms of salinity (calculated using the equation of Potter *et al.* [1978]) are shown alongside the oxygen isotope data in Figure 7. The data are summarized in Table 1. The uniformity of  $T_h$  described above is clearly apparent in Figure 6, which shows that there is no significant variation with paragenetic stage, although small variations in the mean and mode of each population, within the range 125°-140°C, can be seen in Table 1. At no point can primary and secondary inclusion populations be distinguished on the basis of  $T_h$ . A small number of inclusions in the NLQ and breccia matrix quartz show higher  $T_h$ , from 181°-228°C, and a few such inclusions occur also in younger quartz generations.

In the NLQ breccia matrix and the first stage of fracture-filling vuggy quartz (stages 2 and 4) the primary inclusion salinity is relatively high, predominantly between 10 and 13 wt. % NaCl eq. In the coarse-grained vuggy quartz (stage 5a) and the second generation of fine-grained vuggy quartz (stage 5b) two salinity populations are present, one extending from



**Figure 6.** Histograms of homogenization temperature inclusions hosted by successive quartz generations. Inclusions were not observed in stage 6 quartz. Note the remarkably uniform homogenization temperatures.

10 to 15 wt % NaCl eq and a second extending from 2 to 8 wt % NaCl eq. The lower salinity population is more marked, occurring as both primary and secondary inclusions in the fine grained vuggy quartz (stage 5b). Although there are generally too few inclusions within individual crystals to permit

unequivocal demonstration of any trends of fluid variation during quartz growth, low-salinity fluids appear to be more important in the outermost part of the coarse vuggy quartz (stage 5a), suggesting a change in dominant fluid salinity during the growth of this stage. The entire range of inclusion salinities occurs as secondary inclusions within the earliest, NLQ quartz type.

## 6. Stable Isotope Analysis

The results of stable oxygen isotope analysis of quartz are shown in Figure 7 alongside the data on fluid inclusion salinity and are summarized along with the fluid inclusion data in Table 1. An example of the relationships among quartz generations determined from CL, the distribution of higher- and lower-salinity fluid inclusions, and the  $\delta^{18}\text{O}$  values of fragments from a single piece of thick section are illustrated in Figure 8. The  $\delta^{18}\text{O}$  analyses of the NLQ fragments and the associated fracture fill and breccia matrix range from 10‰-13.5‰ but probably do not represent the composition of these quartz stages exactly. Quartz from fresh granite in the EPS-1 core has a composition of ~10‰ [Yardley *et al.*, 1995]. Even at the fine scale of spatial resolution possible with the laser technique, analyzed NLQ fragments will include crack fill of later material, likely to lead to overestimates of the  $\delta^{18}\text{O}$  value, while the breccia matrix samples were likewise probably contaminated with light NLQ fragments. Both the microcrystalline quartz and the vuggy quartz (stages 3 and 4) are heavier and show relatively wide ranges in  $\delta^{18}\text{O}$  (15-18‰ and 14-17.5‰, respectively). Quartz from the central vuggy zone of the vein is lighter than this and exhibits a much narrower range of values, with the coarse- and fine-grained vuggy quartz and the second generation of microcrystalline quartz all lying in the range 12.5‰-14‰. The narrower range of data for stages 5a and 5b may, in part, reflect the ease of obtaining pure separates of these generations.

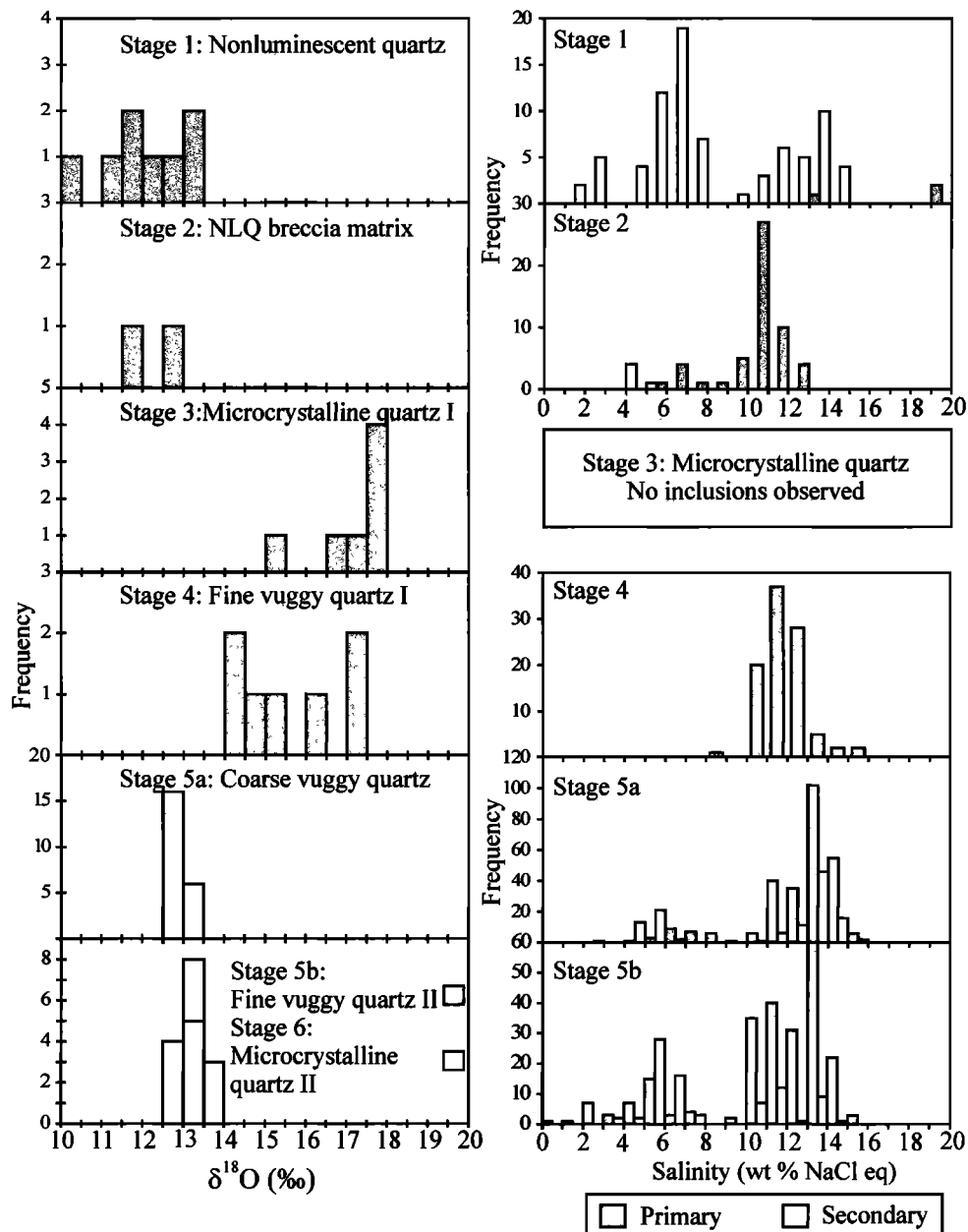
In order to test the homogeneity of the coarse vuggy quartz, a traverse was analyzed across a separate part of the vein using the Cameca ion microprobe at Edinburgh University [Graham *et al.*, 1996; Valley & Graham, 1996]. Results have a relatively poor precision (~1‰;  $1\sigma$ ) but have a spatial resolution of only 20  $\mu\text{m}$  and thus can identify small-scale heterogeneities. The data are shown in Table 2, and it is clear that there are no significant compositional variations, either systematic or oscillatory, within the stage 5a quartz (in marked contrast to most material that has been investigated by the ion probe).

## 7. Discussion and Interpretation

### 7.1. The Pressure and Temperature of Fluid Flow

The data presented above clearly indicate that, as shown by Dubois *et al.* [1996], the temperature and pressure conditions of hydrothermal flow in the Soultz granite have remained remarkably constant throughout the history of fracturing, alteration, and flow from the first development of the quartz veins to the present day. Isochores calculated for the modal salinity of both salinity groupings in each of the quartz generations are shown in Figure 9. The isochores were calculated using the MacFIncor program of Brown and Hagemann [1994] with the equation of state for H<sub>2</sub>O-NaCl from Zhang and Frantz [1987]. Taking a fluid pressure in the





**Figure 7.** Histograms of oxygen isotopic compositions and the corresponding fluid inclusion salinities determined for successive quartz generations. Inclusions were not observed in stage 6 quartz. Note that the large shifts in  $\delta^{18}\text{O}$  do not correlate with the main variation in fluid salinity.

fracture at 2174 m of 215 bars (i.e., near hydrostatic) gives model trapping temperatures in the range 138°-150°C, which is very close to the present temperature at this depth. The majority of the fluid inclusion  $T_h$  values could have been produced by variations in the fluid temperature of only 5°-10°C, (or, much less likely, by much larger variations in the fluid pressure of ~100-200 bars). It is notable that modern fluids in the Soultz granite at 1820 m in the nearby GPK-1 borehole had temperatures of ~137 °C, very close to the lower end of the range reported here from fluid inclusions.

The significant number of inclusions that homogenize above 145°C deserve some comment. They may reflect genuinely higher-temperature conditions during growth, or could have resulted from necking or modification of the fluid inclusions after trapping. We observed no evidence for

necking, and furthermore, if these values result from secondary resetting and leakage, the temperature must still have been higher at the time of leakage than is the case today. The measurements are reproducible and are not therefore an artifact of leakage during measurement. In many cases (secondary inclusions in NLQ quartz) it could be argued that the high-temperature inclusions formed prior to the initiation of the present hydrothermal system, but some high values are recorded from younger quartz generations. It is therefore likely that in some instances they result from short-lived periods of movement of hotter fluids through the fracture network, possibly in response to seismicity [cf. *Muir Wood and King, 1993*]. This suggestion is also consistent with the occurrence of a few veins elsewhere in the Soultz granite core that are dominated by high-temperature inclusions [*Meere et*

**Table 1.** Summary of Fluid Inclusion Microthermometric Data and Oxygen Isotope Data From Quartz From the Saultz Vein Sample at 2174 m

Quartz Stage	Fluid Inclusion Microthermometry						Oxygen Isotope Analyses, $\delta^{18}\text{O}$ in ‰ relative to SMOW				
	Comments	Salinity, wt % NaCl eq			Th, °C			n	Range	Mean	$\pm 2\sigma$
		n	Range	Mode	Range	Mode					
1. Nonluminescent quartz	secondary?	48	1.9-8.0	6.1	125-228	131	8	10.04-13.22	12.07	2.14	
		28	10.2-14.3	13	110-214	129					
2. Breccia matrix	primary	6	5.9-7.6	6.1	181-193	193	2	11.77-12.91	12.34	1.62	
	primary	46	11.7-14.9	12.9	115-184	134					
	secondary	5	4.8-5.2	4.9	137-143	...					
3. Microcrystalline quartz I	...	...	...	...	...	...	7	15.02-17.83	17.09	2.00	
4. Fine vuggy quartz I	primary	98	8.3-15.5	11.2	111-223	136	6	14.09-17.12	15.81	2.52	
5a. Coarse vuggy quartz	primary	26	4.9-8.8	6.8	126-149	131	22	12.61-13.26	12.93	0.30	
	primary	246	9.8-15.7	13.4	106-191	135					
	secondary	37	2.6-6.3	5.2	112-138	138					
	secondary	89	10.8-15.1	13.7	99-202	129					
5b. Fine vuggy quartz II	primary	71	0.9-8.2	4.2	99-200	140	13	12.78-14.12	13.30	0.84	
	primary	248	9.6-15.5	11.8	106-165	128					
	secondary	51	3.1-7.3	5.2	114-143	142					
	secondary	35	10.4-14.8	14.0	117-142	126					
6. Microcrystalline quartz II	...	...	...	...	...	...	3	13.12-13.21	13.15	0.10	

*al.*, 1995] and with the evidence for higher temperatures than those now found during formation of tosdite alteration [Ledestert *et al.*, 1996].

## 7.2. The Variation of Fluid Source with Time.

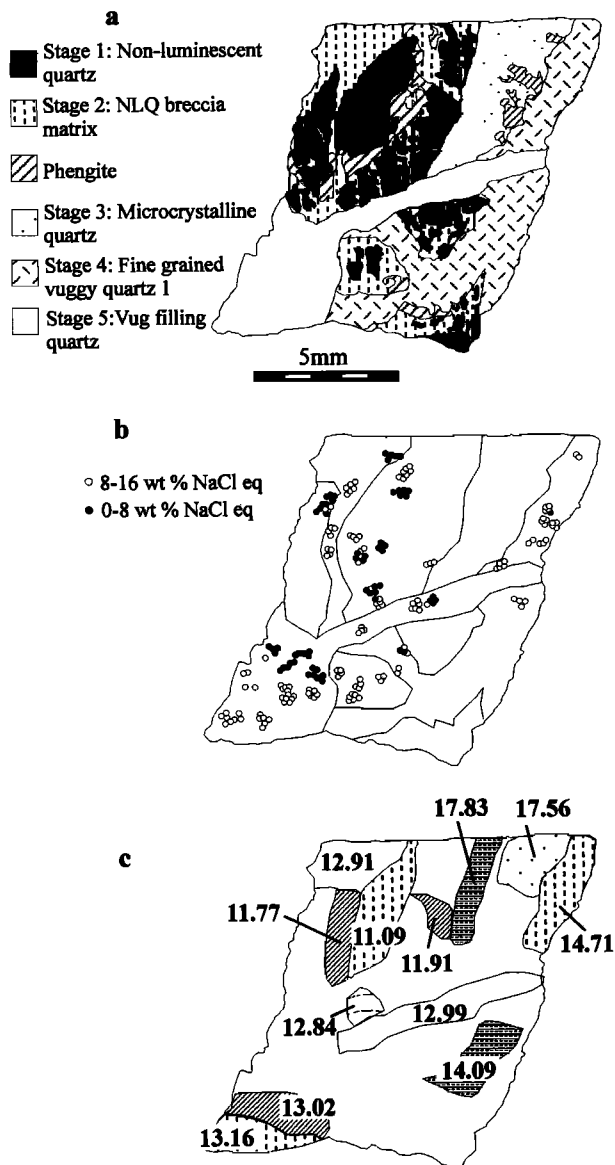
The oxygen isotope data from this study clearly differentiate at least three periods of quartz growth. In stages 1 and 2, light values of  $\delta^{18}\text{O}$ , from 10.1‰-13.2‰, typify the nonluminescent quartz and its associated fracture fill. In stages 3 and 4 the heaviest values of  $\delta^{18}\text{O}$ , from 14.1‰-17.8‰, occur in the first stage of microcrystalline quartz and in fine-grained vug-filling quartz. In stages 5 and 6, intermediate values from  $\delta^{18}\text{O}$ , 12.6‰-14.1‰, characterize the coarse-grained vuggy quartz and the second generations of fine-grained vuggy quartz and microcrystalline quartz. These results are in close agreement with the data from other veins in the EPS-1 core summarized by Yardley *et al.* [1995] but are all lighter than a single measurement of hydrothermal vein quartz from GPK-1 of 19.3‰ reported by Fouillac and Genter [1991]. Since the two studies yielded similar results for granite quartz (below), there is no reason to suppose that the differences in the data are not real, but it now appears that the composition for hydrothermal quartz reported by Fouillac and Genter [1991] is not typical, and therefore their interpretations based on it must be revised in the light of the new results.

The light end of the range of values for stage 1 corresponds closely to that analyzed for the host granite quartz phenocrysts (~10.0‰) [e.g. Fouillac and Genter, 1991; Yardley *et al.*, 1995]. Along with the association with mica, monazite, and zircon, this suggests that the oldest quartz in the paragenesis comprises brecciated fragments from the granite, unaffected by hydrothermal activity. The heavier values of some analyzed fragments are almost certainly due to the presence of fractures filled with stage 2 quartz. The composition of the subsequent,

hydrothermal quartz reflects the isotopic composition of the hydrothermal fluid and the temperature of growth. Since the temperature has been shown from fluid inclusion studies to be very constant, with no systematic trends, the changes in quartz composition must reflect changes in the fluid. We have therefore calculated the composition of fluid in equilibrium with the analyzed hydrothermal quartz at a temperature of 150°C, using the fractionation factor of Zhang *et al.* [1989], extrapolated to low temperatures. Because of the variable salinity of the hydrothermal fluid, it is necessary to take into account the possible effect of dissolved salts on water activity and hence the mineral - water oxygen isotope fractionation factor [e.g., Truesdell, 1974; Horita *et al.*, 1993a, b, 1995]. Calculation of these effects at 150°C using the equation of Horita *et al.* [1995] and assuming an NaCl dominated fluid indicates a correction of <0.1‰ at both 5 and 13 wt % NaCl. This is less than the likely 2 $\sigma$  error in the analyses and so has little effect on the inferred fluid composition.

The results are shown in Figure 10, together with the composition of the modern fluid at Saultz [Pauwels *et al.*, 1993] and, for comparison, a deep fluid from Bühl (Figure 1), which was the heaviest Rhine Graben fluid reported by Pauwels *et al.* [1993]. Thermal waters in the Rhine Graben yield much lighter compositions dominated by a meteoric component [Pauwels *et al.*, 1993]. It can be seen that the composition of the fluid that precipitated the youngest quartz generations, stages 5 and 6, closely resembles that of the modern fluid, while the composition of fluids in equilibrium with stage 3 and 4 quartz was several per mil heavier than this. The initial NLQ breccia matrix was also apparently formed from fluid similar to that present today.

Relatively heavy fluids, often with  $\delta^{18}\text{O} > 0\text{‰}$ , are typical of sediment-hosted brines which have equilibrated with authigenic minerals in deep basins [e.g. Fontes and Matray,



**Figure 8.** Part of the sample illustrated in Figure 2 (see Figure 2b for location), showing (a) the quartz generations identified in CL; (b) the distribution of higher and lower salinity fluid inclusions and (c) the fragments broken off for oxygen isotope analysis and their compositions.

1993a, b], and indeed the Bühl hole (fluid plotted on Figure 10a) produces from Buntsandstein at 2540 m depth. The origin of the fluids at  $\sim -2.3\text{‰}$  is also likely to be controlled by mineral equilibria because this composition has clearly been important throughout at least one extended period of hydrothermal activity. Figure 10 shows the range of possible compositions for water equilibrated with Soultz granite feldspar [Yardley *et al.*, 1995] over the temperature range  $100^{\circ}$ - $250^{\circ}\text{C}$ , calculated using the fractionation factor of Bottinga and Javoy [1973] and correcting the calculated fluid composition for a salinity of 13 wt % NaCl (approximately that of the high-salinity fluid inclusion population) using the equation of Horita *et al.* [1995]. Feldspar is the most reactive phase in the granite and is therefore likely to dictate the composition of fluid that reacts with it [Sardini *et al.*, 1996]. It is clear that fluids equilibrated with the granite feldspar at a

temperature  $20^{\circ}$ - $30^{\circ}\text{C}$  higher than that of quartz precipitation in the veins will have an isotopic composition identical to that of the present fluid and to that which precipitated the younger quartz generations.

It is also apparent from Figure 10 that the heaviest fluids, responsible for stage 3 and 4 quartz, could only result from equilibrium with granite if temperatures were in excess of  $250^{\circ}\text{C}$ . Such large temperature changes are consistent with neither the alteration patterns nor the fluid inclusion results. It seems more likely that they resulted from exchange with sediments at temperatures closer to those observed or inferred from the geothermometers [cf. Dubois *et al.*, 1996; Kominou and Yardley, 1997].

In summary, we interpret the earliest quartz generation in the vein to comprise fragments of original granite quartz [cf. Slater *et al.*, 1993]. The early stages of growth of fine-grained and microcrystalline quartz (stages 3 and 4) grew from an isotopically heavier water, probably a sedimentary basinal brine. The younger stages of vein quartz grew from a fluid which had the same oxygen isotopic composition as the present fluid, despite differences in salinity, and was at the present field temperature. This conclusion differs from that of Fouillac and Genter [1991], who argued on the basis of isotopic data from the GPK-1 core that only calcite from the producing level at 1820 m had formed in equilibrium with the modern fluid because our much more extensive data set extends the range of measured hydrothermal quartz compositions. Both studies have, however, found evidence for influx of an isotopically heavy water at certain times.

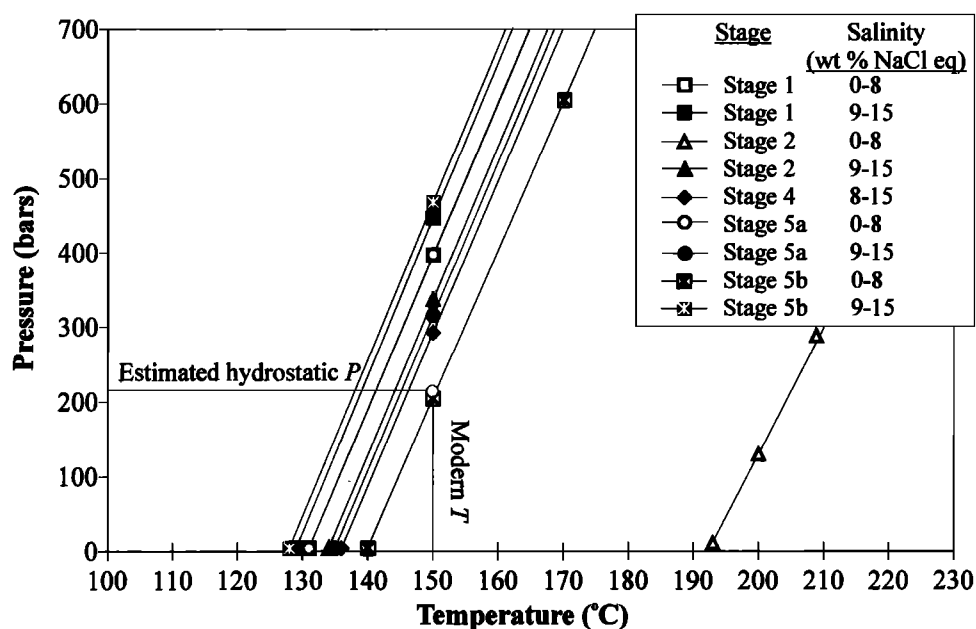
### 7.3. Reconciling the Evidence of Fluid Inclusions and Oxygen Isotopes: The Evolution of Fluids in the Soultz System

To understand how the fluid flow system has evolved in the region around Soultz, it is necessary to reconcile several different types of evidence which yield apparently contradictory results. Different fluid components may respond differently during the same sequence of processes, according to how conservative they are. The halogens, Cl and Br, are conservative except in the presence of halite. They dictate the total dissolved load of the fluid and provide a tracer for the source of salinity because they are not involved in exchange reactions with granitic wall rocks or precipitated in any vein

**Table 2.** Traverses of Oxygen Isotope Analyses by Ion Microprobe Across Coarse-Grained Vuggy Quartz Crystals

Traverse A		Traverse B	
X, $\mu\text{m}$	$\delta^{18}\text{O}$ , ‰	X, $\mu\text{m}$	$\delta^{18}\text{O}$ , ‰
60	12.7	0	14.1
75	16.3	158	12.4
162	14.2	274	12.9
281	13.8	366	11.6
522	12.6	572	13.0
630	15.1	660	11.3
746	15.2	700	13.8
833	14.7	759	12.9
920	14.1	860	13.0
1007	14.4	1816	12.4
1124	13.8		

Grain edge at  $0\mu\text{m}$ ; grain center at  $1010\mu\text{m}$ .



**Figure 9.** Isochores constructed for the modal homogenization temperatures of primary fluid inclusions from each of the quartz generations (see Figure 6). Secondary inclusions are plotted for the nonluminescent quartz (stage 1) as these dominate the population. Secondary inclusions for other generations define very similar isochores to the primary inclusions. Note the close correspondence to the present day fluid density for all but the high  $T_h$  inclusions from stage 2.

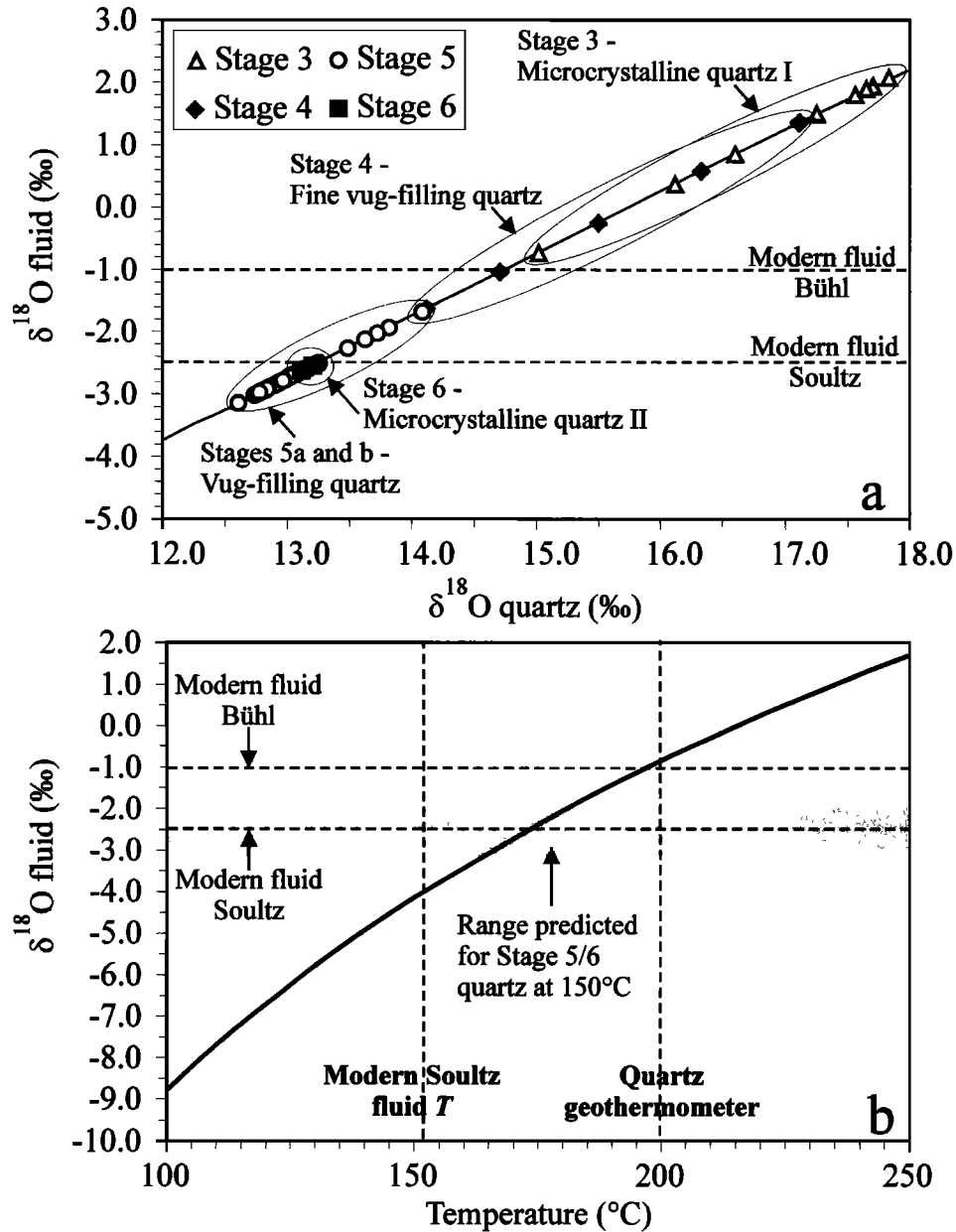
minerals. In contrast, if fluids are slow moving, they may exchange oxygen extensively with many minerals at the temperatures of interest for this study.

Hydrological models of fluid flow in the Rhine Graben carried out by *Clauser [1989]* and *Person and Garven [1989, 1992]* are not strictly applicable to the Soultz problem, as they assumed very low permeabilities in the granite basement, leading to predictions of no flow in the basement. They do, however, indicate the general flow pattern within the graben and suggest a flow of fluids from the thickest regions of the sedimentary pile both perpendicular to the Rhine Graben axis from the margins toward the Soultz Horst and parallel to the axis in a northward direction. This could result in a range of flow paths and residence times in the granite. *Kominou and Yardley [1997]* argued on geochemical grounds that the alteration seen around veins in the Soultz granite requires that fluids from sedimentary rocks in the thickest part of the graben moved into the granite while still moving up temperature.

More recently the two dimensional conductive-convective heat transfer model of *Flores and Royer [1993]* and *Le Carlier et al. [1994]* predicted vertical convection of fluid between sedimentary cover and fractured basement down to a depth of 4000 m, relating to three hydrothermal circulation systems within the Soultz area. The first is located in the eastern part of the graben and involves flow of deep fluids out from the thickest regions of the sedimentary graben fill toward the edge of the graben near Baden-Baden. The second one extends from the Rhine Graben axis westward to the Soultz horst and does not exchange with surface fluids. It is a closed cell containing trapped fluids of probable sedimentary origin and redistributes heat, with the Soultz horst at the top of its upwelling portion. The third and smallest cell originates in the

western part of the graben and extends east to Hochwald, northwest of Soultz. In this model the Soultz horst could be a site of upwelling of fluids from either the central or western cells, and variation in their respective contributions could account for the variations in salinity recorded by the fluid inclusions in EPS-1 [*Dubois et al., 1996*]. However, it does not necessarily account for the uniform homogenization temperatures for the different fluids.

The pattern of fluid inclusion salinities reported in Figure 7 indicates that the fluid salinity has not simply evolved from a more saline composition in the past to a relatively dilute one today. Instead, there is evidence for relatively low salinity fluids during stage 2 and again during stages 5a and 5b. While the coarse vuggy quartz appears to show a trend to lower salinity during growth, there are some higher-salinity fluids in the following stage. Furthermore, the present fluid has a salinity intermediate between the extremes recorded by fluid inclusions. We can confirm that the fluid system at Soultz is fed by at least two sources of salinity, corresponding to either mixing of waters from reservoirs of higher and lower salinity in differing proportions, or to movement of low-salinity waters through an evaporite-bearing sequence with differing degrees of interaction with halite. In either case it is likely that the salinity of fluid entering the Soultz flow system is established at an early stage along the flow path, during heating, because it is clear from Figure 5 that there is no temperature difference between fluids of different salinities. This appears to preclude the possibility that the salinity range observed is simply the result of the mixing of meteoric waters from the sides of the graben with deep brines from within it. Different degrees of mixing arising because of the preservation of density contrasts between high- and low-salinity fluids could also contribute to the variation in fluid salinity but is unlikely to have been a

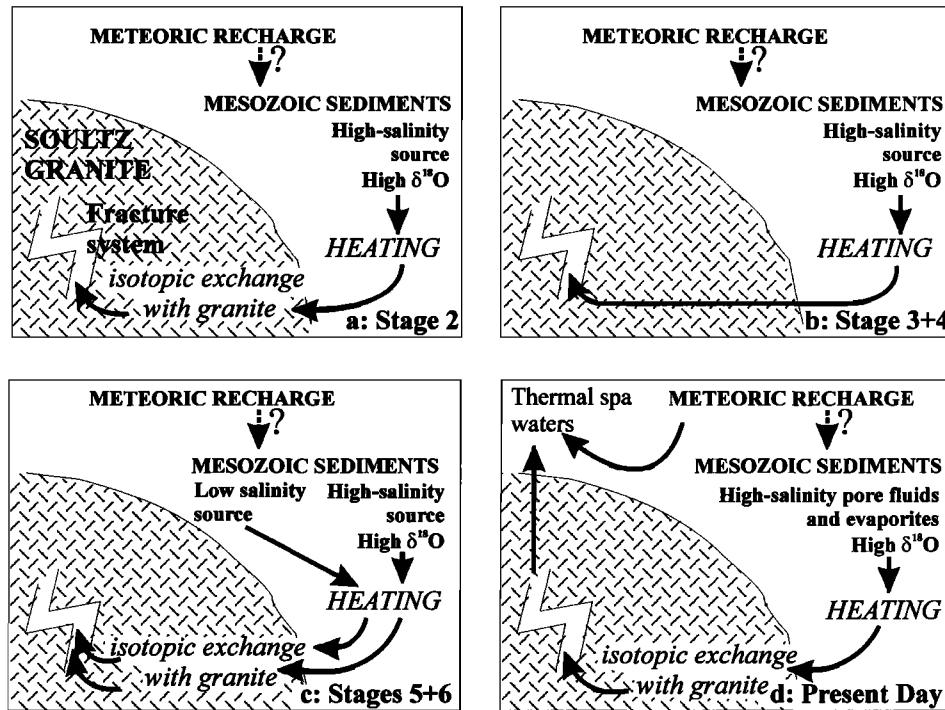


**Figure 10.** Interpretation of the oxygen isotope results. (a) Curve calculated to show compositions of quartz and fluid coexisting in equilibrium at 150°C. This has been annotated with data points from the analyzed quartz grains. Horizontal lines are examples of modern fluid compositions from the Rhine Graben, from Pauwels et al. (1993). The youngest quartz generations are close to equilibrium with the modern fluid at Soultz, while some earlier quartz grew from a heavier fluid. (b) Curve calculated to show the composition of fluid equilibrated with feldspar from the Soultz granite, as a function of temperature. The modern fluid composition is close to equilibrium with feldspar at a temperature intermediate between the measured downhole temperature and the quartz geothermometer temperature for the same analyzed waters, reported by Pauwels et al. (1993).

major effect as the homogenization temperatures of fluid inclusions indicate only minor density differences between the two fluid populations preserved in the vein.

Further evidence to indicate that fluids have a long history of water-rock interaction, regardless of salinity, comes from the oxygen isotope data. Perhaps the most important point to be made here is that the changes in isotopic composition of the vein quartz do not correspond in time to changes in fluid inclusion salinity (Figure 7). None of the oxygen data indicate a meteoric input, in contrast to analyzed shallow thermal

waters [Pauwels et al., 1993]. Stage 4 quartz grew from high-salinity, heavy fluids, which gave way to a lighter, granite-equilibrated fluid at the onset of growth of the coarse vuggy quartz (stage 5a). However, most of the inclusions in this quartz generation are of high salinity. Despite the evidence for a drop in fluid salinity during the final stages of growth of these crystals they are isotopically homogeneous (Table 2). The shift in oxygen isotopic composition does not therefore reflect the influx of fluid from a different source, rather the same, high-salinity fluid changed the way it flowed through



**Figure 11.** (a)-(c) Schematic representation of the fluid sources and the processes affecting fluid composition for the vein investigated. The arrows indicate possible fluid inputs to the Soutz granite system and are not intended to depict specific flow paths. Mesozoic sediments are the likely immediate source of fluids that infiltrate the granite, having first been heated in deeper parts of the graben. Once they have passed into the crystalline basement, fluids have interacted with granite feldspar to varying degrees at different times. (d) Summary of possible inputs to the modern fluid based on the work of *Pauwels et al.*, (1993). They interpreted the fluid salinity as resulting from the mixing of a primary brine with a more dilute fluid, followed by the dissolution of halite. A meteoric water signature has only been detected in waters from modern thermal spas but is a possible source for low salinity recharge.

the system in such a way as to permit more extensive interaction with granite while not perturbing the thermal structure. This might be achieved by, for example, the development of more, narrower fractures for flow, giving rise to an increased surface area of fracture wall or a lengthening of the flow path through granite from the adjacent, younger sediments. Fluid has been isotopically equilibrated with the granite from the onset of stage 5a to the present, but a considerable range of fluid salinities have been preserved in this time. Figure 11 is a schematic summary of the constraints on fluid flow in the Soutz system deduced from the evidence presented here and consistent with previous geochemical studies by *Pauwels et al.* [1993] and *Kominou and Yardley* [1997].

## 8. Conclusions

The quartz vein that coincides with the main fluid-producing level in the Soutz granite in drill hole EPS-1, has formed during a protracted history of fluid circulation involving a number of fracturing and self-sealing events. The most recent stages of vein fill formed from a fluid with a similar oxygen isotopic composition to that of the modern fluid and at the same temperature. Coupled with the observation that the modern fluid is saturated with respect to quartz [*Pauwels et al.*, 1993], this suggests that quartz vein growth may be active at the present day.

Despite large variations in the fluid composition as the vein developed the fluid temperature and pressure appear to have varied only slightly from the modern conditions (the temperature is 150°C and fluid pressure is ~215 bars). Nevertheless, some inclusions of less dense water do occur and may reflect short pulses of flow of hotter water through the system, possibly in response to earthquakes. The development of the vein can be summarized as follows:

1. The Soutz granite fractures initially and brecciated quartz fragments are included within the vein cavity (the nonluminescent quartz). These fractures were sealed in hydrothermal quartz precipitated from saline fluids, close to being isotopically equilibrated with granite feldspars. The present thermal structure was already established at this stage.

2. The fine grained to microcrystalline quartz is precipitated, followed by a second fracturing event and the filling of these fractures with the first generation of euhedral, vug filling quartz. The fluids during this period appear to have been of higher salinity than the modern fluid (~10-15 wt % NaCl eq) and to have moved through the granite from the Mesozoic sedimentary sequence too quickly to have attained isotopic equilibrium with the granite feldspar.

3. A third fracturing event took place and was sealed by euhedral vug-filling quartz and its finer-grained equivalents. The fluid at this stage was isotopically similar to the modern fluid, having equilibrated with granite as it moved through it at temperatures near 175°C, but showed a range of salinities, both higher and lower than that of the modern fluid.

4. The final growth of quartz, lining cavities in the modern vein, is too fine grained to preserve fluid inclusions but is isotopically equilibrated with the modern fluid. It would appear likely that it was continuing to grow up to the time of drilling.

**Acknowledgments.** This work has been supported in part by the European Community Joule II programme, project J0U2-CT93-0318, and by Institut National des Sciences de l'Univers Project DBT-INSU "Fluids in the Crust." Oxygen isotope analysis at the University of Wisconsin was supported by NSF (EAR9304372) and DOE (93ER14389); we are also indebted to M. Spicuzza for his assistance. We are indebted to J. Craven for ion microprobe analyses, made at the University of Edinburgh, and to E. Condliffe, Leeds, for assistance with SEM imaging. T. Lutz, T. Labotka and J. Sissons are thanked for their constructive reviews.

## References

- Aquilina, L., and M. Brach, Characterization of Soultz hydrochemical system: WELCOM (well chemical on-line monitoring) applied to deepening of GPK-1 borehole, *Geotherm. Sci. Tech.*, **4**, 239-251, 1995.
- Boiron, M. C., S. Essarraj, E. Sellier, M. Cathelineau, M. Lespinasse, and B. Poty, Identification of fluid inclusions in relation to their host microstructural domains in quartz by cathodoluminescence, *Geochim. Cosmochim. Acta*, **56**, 175-185, 1992.
- Bottinga, Y. and M. Javoy, Comments on oxygen isotope geothermometry, *Earth Planet. Sci. Lett.*, **20**, 250-265, 1973.
- Brace, W.F., Permeability of crystalline and argillaceous rocks, *Int. J. Rock Mech. Min. Sci.*, **17**, 241-251, 1980.
- Bresee, J.C. (Ed.), Geothermal energy in Europe: The Soultz Hot Dry Rock Project, 309pp, Gordon and Breach, Newark, N.J., 1992.
- Brown, P. E., and S. G. Hagemann, MacFlincor: A computer program for fluid inclusion data reduction and manipulation, in *Fluid Inclusions in Minerals: Methods and Applications*, edited by B. De Vivo and M. L. Frezzotti, pp. 231-250, Virginia Polytechnic Institute Press, 1994.
- Clouser, C., Conductive and convective heat flow components in the Rheingraben and implications for the deep permeability distribution, in *Hydrogeological Regimes and Their Subsurface Thermal Effects*, *Geophys. Monogr. Ser.*, vol. 47, edited by A. E. Beck, G. Garven and L. Stegenar pp. 59-64, A.G.U. Washington, D.C., 1989.
- Dubois, M., M. A. Ougougdal, P. Meere, J. J. Royer, M. C. Boiron, and M. Cathelineau, Temperature of Palaeo- to modern self sealing within a continental rift basin: The fluid inclusion data (Soultz-sous-Forêts, Rhine Graben, France). *Eur. J. Mineral.*, **8**, 1065-1080, 1996.
- Elsass, P., L. Aquilina, A. Beauce, Y. Benderitter, A. Genter, and H. Pauwels, Deep structures of the Soultz-sous-Forêts HDR site, paper presented at World Geothermal Congress, Florence, Italy, 1995.
- Flores, E.L., and J.J. Royer, Convective heat transfer around the Soultz-sous-Forêts geothermal site (Rhine graben), paper presented at VIth International Symposium on Continental Deep Drilling Programs, Paris, 1993.
- Fontes, J. C., and J. M. Matray, Geochemistry and origin of formation brines from the Paris Basin, France, 1, Brines associated with Triassic salts, *Chem. Geol.*, **109**, 149-175, 1993a.
- Fontes, J. C. and J. M. Matray, Geochemistry and origin of formation brines from the Paris Basin, France, 2, Saline solutions associated with oil fields, *Chem. Geol.*, **109**, 177-200, 1993b.
- Fouillac, A. M. and A. Genter, An O, D, C isotopic study of water/rock interactions in the Soultz-sous-Forêts granite, *Geotherm. Sci. Tech.*, **3**, 105-117, 1991.
- Fritz, P. and S.K. Frappe, Saline water and gases in crystalline rocks, *Geol. Assoc. Can. Spec. Pap.*, **33**, 259pp, 1987.
- Genter, A., H. Traîneau, C. Dezayes, B. Ledésert, A. Meunier, and T. Villemin, Caractérisation lithologique et structurale dans le forage GPK-1 entre 2000 et 3600 m (Soultz-sous-Forêts, France), in Principaux résultats scientifiques et techniques du B.R.G.M.-1992/1993, Rep. RS 2949, pp.139-141, Bur. De Rech. Geol. Et Min., Orléans, France, 1993.
- Gérard, A., and O. Kappelmeyer, The Soultz-sous-Forêts project and its specific characteristics with respect to the present state of experiments with HDR, *Geothermics*, **16**, 393-399, 1987.
- Graham, C.M., J.W. Valley, and B.L. Winter, Ion microprobe analysis of  $^{18}\text{O}/^{16}\text{O}$  in authigenic and detrital quartz in the St. Peter sandstone, Michigan basin and Wisconsin Arch, USA: Contrasting diagenetic histories, *Geochim. Cosmochim. Acta*, **60**, 5101-5116, 1996.
- Horita, J., D.J. Wesolowski, and D.R. Cole, The activity-composition relationship of oxygen and hydrogen isotopes in aqueous salt solutions, I, Vapour-liquid water equilibration of single salt solutions from 50 to 100°C, *Geochim. Cosmochim. Acta*, **57**, 2797-2817, 1993a.
- Horita, J., D.R. Cole, and D.J. Wesolowski, The activity-composition relationship of oxygen and hydrogen isotopes in aqueous salt solutions, II, Vapour-liquid water equilibration of mixed salt solutions from 50-100°C and geochemical implications, *Geochim. Cosmochim. Acta*, **57**, 4703-4711, 1993b.
- Horita, J., D.R. Cole, and D.J. Wesolowski, The activity-composition relationship of oxygen and hydrogen isotopes in aqueous salt solutions, III, Vapour-liquid water equilibration of NaCl solutions to 350°C, *Geochim. Cosmochim. Acta*, **59**, 1139-1151, 1995.
- Illies, J.H., and G. Greiner, Rhinegraben and the Alpine system, *Geol. Soc. Am. Bull.*, **89**, 770-782, 1978.
- Kominou, A., and B.W.D. Yardley, Fluid-rock interactions in the Rhine Graben: A thermodynamic model of the hydrothermal alteration observed in deep drilling, *Geochim. Cosmochim. Acta*, **61**, 515-531, 1997.
- Le Carlier, C., J.J. Royer, and E.L. Flores, Convective heat transfer at Soultz-sous-Forêts geothermal site: Implications for oil potential, *First Break*, **12**, 553-560, 1994.
- Ledésert, B., J. Dubois, A. Genter, and A. Meunier, Fractal analysis of fractures applied to the Soultz-sous-Forêts hot dry rock geothermal program, *J. Volcanol. Geotherm. Res.*, **57**, 1-17, 1993.
- Ledésert, B., J. Joffre, A. Ambles, P. Sardini, A. Genter, and A. Meunier, Organic matter in the Soultz HDR granitic thermal heat exchanger (France): A natural tracer of fluid circulations between the basement and its sedimentary cover, *J. Volcanol. Geotherm. Res.*, **70**, 235-253, 1996.
- Meere, P.A., M. Cathelineau, M. Dubois, M. Ayt-Ougougdal, and J.J. Royer, Are quartz veins forming under Strasbourg today? A fluid inclusion study, *Terra Nova*, **7**, 185, 1995.
- Muir Wood, R., and G.C.P. King, Hydrologic signatures of earthquake strain, *J. Geophys. Res.*, **98**, 22,035-22,068, 1993.
- Pauwels H., C. Fouillac, and A.-M. Fouillac, Chemistry and isotopes of deep geothermal saline fluids in the Upper Rhine Graben: Origin of compounds and water-rock interactions. *Geochim. Cosmochim. Acta*, **57**, 2737-2749, 1993.
- Person, M. and G. Garven, Hydrologic constraints on the thermal evolution of the Rhine Graben, In *Hydrogeological Regimes and Their Subsurface Thermal Effects*, *Geophys. Monogr. Ser.*, vol. 47, edited by A. E. Beck, G. Garven, and L. Stegerian, pp. 35-58, A. G. U., Washington, D.C., 1989.
- Person, M. and G. Garven, Hydrologic constraints on petroleum generation within continental rift basins: Theory and application to the Rhine Graben, *AAPG Bull.*, **76**, 468-488, 1992.
- Potter, R. W. II, M. A. Clyne, and D. L. Brown, Freezing point depression of aqueous sodium chloride solutions, *Econ. Geol.*, **73**, 284-285, 1978.
- Roedder E., Metastable superheated ice in liquid water inclusions under high negative pressure, *Science*, **155**, 1413-1417, 1967.
- Sardini, P., B. Ledésert, and G. Touchard, Quantification of microscopic porous networks by image analysis and measurements of permeability in the Soultz-sous-Forêts granite (Alsace, France), in *Fluid Flow and Transport in Rocks*, edited by B. Jamveit and B.W.D. Yardley, pp.171-189, Chapman and Hall, New York, 1996.
- Slater, D.J., B.W.D. Yardley, B. Spiro, and R.J. Knipe, Incipient deformation and metamorphism in the Variscides of SW Dyfed, Wales: First steps towards isotopic equilibrium, *J. Metamorph. Geol.*, **12**, 237-248, 1993.
- Spicuzza, M.J., J.W. Valley, M.J. Kohn, J.P. Girard, and A.M. Fouillac, The rapid heating, defocused beam technique: A CO<sub>2</sub>-laser-based method for highly precise and accurate determination of delta O-18 values of quartz, *Chem. Geol.*, **144**, 195-203, 1998.

- Traineau, H., A. Genter, J. P. Cautru, H. Fabriol, and P. Chevremont, Petrography of the granite massif from drill cutting analysis and well log interpretation in the geothermal HDR borehole GPK 1 (Soultz, Alsace, France), *Geotherm. Sci. Tech.* 3, 1-29, 1991.
- Truesdell, A.H., Oxygen isotope activities and concentrations in aqueous salt solutions at elevated temperatures: consequences for isotope geochemistry, *Earth Planet. Sci. Lett.*, 23, 387-396, 1974.
- Valley, J.W., and C.M. Graham, Ion microprobe analysis of oxygen isotope ratios in quartz from Skye granite: Healed micro-cracks, fluid flow and hydrothermal exchange, *Contrib. Mineral. Petrol.*, 124, 225-234, 1996.
- Valley, J. W., N. Kitchen, M. J. Kohn, C. R. Niendorf, and M. J. Spicuzza, UWG-2, A garnet standard for oxygen isotope ratios: Strategies for high precision and accuracy with laser heating, *Geochim. Cosmochim. Acta*, 59, 5223-5231, 1995.
- Villemin T., F. Alvarez, and J. Angelier, The Rhine Graben: Extension, subsidence and shoulder uplift, *Tectonophysics*, 128, 47-59, 1986.
- Yardley, B. W. D., P. A. Meere, M. Cathelineau, and J. W. Valley, Are quartz veins forming under Strasbourg today? A stable isotope study of vein quartz from Soultz-sous-Forêts. *Terra Nova Abstr.*, 7, 185, 1995
- Zhang, L. F., J. F. Liu, and Z. S. Chen, Oxygen isotope fractionation in the quartz-water-salt system, *Econ. Geol.*, 84, 1643-1650, 1989.
- Zhang, Y. G., and J. D. Frantz, Determination of homogenisation temperatures and densities of supercritical fluids in the system NaCl-KCl-CaCl<sub>2</sub>-H<sub>2</sub>O using synthetic fluid inclusions, *Chem. Geol.*, 64, 335-350, 1987.
- 
- M. Dubois, Université des Sciences et Technologies de Lille, Unité de Recherche Associée 719, Sédimentologie et Géodynamique, 59653 Villeneuve d'Ascq Cedex, France. (e-mail: Michel.Dubois@univ-lille.fr)
- J. J. Royer and V. Savary, Centre de Recherches Pétrographiques et Géochimiques - Centre National de la Recherche Scientifique, BP 20, 54501 Vandoeuvre les Nancy Cedex, France. (e-mail: royer@ensg.u-nancy.fr)
- M. P. Smith, Department of Mineralogy, The Natural History Museum, Cromwell Road, London SW7 5BD, England, U.K. (e-mail: mars@nhm.ac.uk)
- J. W. Valley, Department of Geology and Geophysics, University of Wisconsin, Madison, WI 53706. (e-mail: valley@geology.wisc.edu)
- B. W. D. Yardley, Department of Earth Sciences, University of Leeds, Leeds LS2 9JT, England, U.K. (e-mail: B.Yardley@earth.leeds.ac.uk)

(Received November 24, 1997; revised June 22, 1998; accepted July 28, 1998)